VARIABLE FLIP ANGLE DESIGN FOR BALANCED SSFP TRANSIENT STATE IMAGING TO IMPROVE HP ^{13}C MRI

Hong Shang[1,2], Peder E.Z. Larson[1,2], Galen Reed[3], Eugene Milshteyn[1,2], Cornelius von Morze[1], Frank Ong[4], Jeremy W. Gordon[1], Jonathan I. Tamir[4], and Daniel B. Vigneron[1]

[1]Radiology and Biomedical Imaging, UCSF, San Francisco, California, United States, [2]UCSF-UC Berkeley Graduate Program in Bioengineering, San Francisco/Berkeley, California, United States, [3]HeartVista, Menlo Park, California, United States, [4]Electrical Engineering and Computer Science, UC Berkeley, Berkeley, California, United States

Purpose Balanced steady-state free precession (bSSFP) sequences offer high SNR efficiency for rapid 2D and 3D ^{1}H MRI. bSSFP has been applied for hyperpolarized (HP) ^{13}C imaging, preserving non-recoverable HP signal efficiently with zero gradient-induced dephasing (1-2). For these applications signal acquisition typically occurs during the transient state, either to reduce waiting time for ^{1}H MR or as the nature of HP ^{13}C MR. For transient state imaging, a constant flip angle (CFA) is no longer optimal since it results in a decaying signal profile. By varying flip angles, it is possible to achieve a uniform signal profile with higher signal strength, which would increase SNR and reduce image blurring. Previous variable flip angle (VFA) schemes have been developed to achieve target signal profile for spins on-resonance with analytical expression (3-4). However, the result is usually sensitive to off-resonance effects. A novel approach of bSSFP VFA design is presented using non-convex optimization with improved off-resonance insensitivity.

Methods and Results Given a specific VFA scheme, signal profile can be calculated based on the Bloch equation in matrix form (5). If a uniform signal profile over a range of off-resonance frequencies is desired, the problem becomes over-determined and can no longer be solved analytically. Here, an optimization approach is proposed to achieve a relatively uniform signal profile within a range of frequencies with flip angle (α) and RF phase (φ) as the optimization variables. The cost function is defined as in equation (1), where $M_{xy,k}/M_{d,k}$ is the actual/desired signal at the k^{th} echo, and f_j is the discrete off-resonance frequency of interest. If k starts from $k_0 > 1$, the RF pulses before k_0 are equivalent to a preparation pulse. This cost function is non-convex but smooth with an analytical expression for the gradient. A gradient descent algorithm is used to calculate a local optimal solution.

$$f_0(\alpha,\varphi) = \sum_{j=1}^{m}\sum_{k=1}^{n}(|M_{xy,k}(\alpha,\varphi,f_j)| - M_{d,k})^2 \qquad (1)$$

HP ^{13}C MR experiments were performed to measure the bSSFP transient state signal profile with the VFA schemes, as a function of both time and off-resonance frequency. Dissolution DNP was performed with a HyperSense polarizer (Oxford Instruments, Oxford, UK). MR experiments were performed on a 3T clinical MRI scanner (GE Healthcare, Waukesha, WI, USA). Dynamic 1D spatial profiles were acquired (bSSFP without phase encoding,TR=10ms) for a HP urea phantom (T1/T2=45s/82ms), using either a CFA (38°) or the proposed VFA scheme, as shown in Fig 1(A). The VFA was designed given T2=86ms, slightly different from the real T2 to simulate non-ideal T2 estimation. Signal profiles for on-resonance spins are shown in Fig 1(B) with the corresponding point spread function in Fig 1(C). A constant gradient was applied during acquisition to simulate off-resonance effects. Measured signal profiles are shown with CFA (Fig 3A) and VFA (Fig 3B), compared to Bloch simulation results (Fig 2).

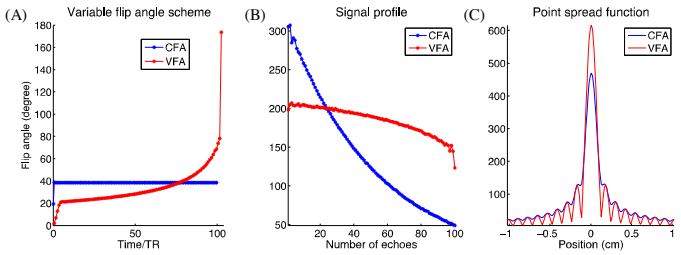

Figure 1. Flip angle scheme (A) for bSSFP sequence including constant flip angle (CFA) and variable flip angle (VFA). The signal profile (B) and the corresponding point spread function(C) were measured for spins on resonance.

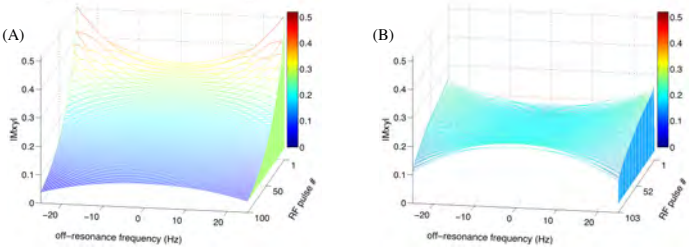

Figure 2. Bloch simulation results of bSSFP transient state signal profile as a function of off-resonance frequency and number of echoes for CFA (A) and VFA (B) schemes.

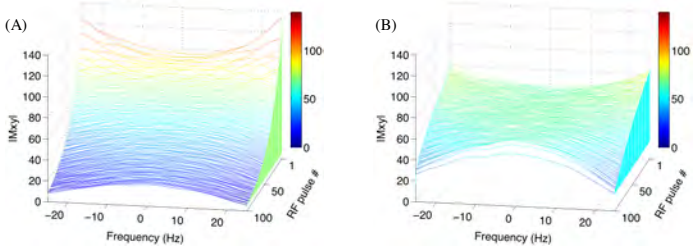

Figure 3. Measured signal profiles as in Figure 2.

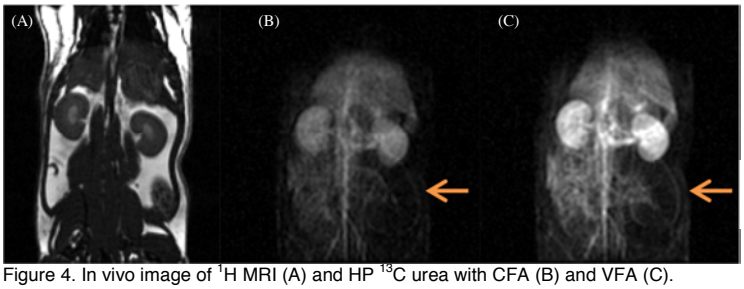

Figure 4. In vivo image of ^{1}H MRI (A) and HP ^{13}C urea with CFA (B) and VFA (C).

A HP ^{13}C in vivo animal study was performed to acquire a 2D image with sequential phase encoding (projection along A/P direction) with either a CFA (68°) or VFA scheme. HP urea was injected with estimated T1/T2 = 45s/280ms (2). Parameters include: TR=10ms, matrix=96×96, FOV=12×12cm. These images are shown in Fig 4, along with the corresponding slice from a 3D bSSFP ^{1}H scan.

Discussion The measured signal profile during the transient state of a bSSFP sequence matches with simulation results. Using the proposed VFA scheme, a uniform signal profile with higher total signal was achieved within targeted off-resonance frequencies of [-25Hz, 25Hz], which covers most of the field inhomogeneity in the application. An animal experiment with VFA showed less blurring along the phase encoding (horizontal) direction. Some small structures were only detected in the VFA image (arrow in Fig 4). SNR measured at left kidney center was 1.8 fold higher with the VFA scheme.

Even though only the magnitude of signal is specified in the cost function, the result has a very uniform phase profile as well (results not shown). The refocusing property is well-known for bSSFP with CFA (6). Our simulation shows that this refocusing property also exists for transient state and VFA with alternating RF phase, which explains the uniform phase profile. The optimization approach can also be expanded for other purposes, such as reducing sensitivity to T1/T2 deviation, maximizing total signal. The limitation of this approach is the larger computation cost and B1 sensitivity.

Conclusion A variable flip angle scheme was designed for bSSFP transient state imaging with improved off-resonance insensitivity by solving a non-convex optimization problem. HP ^{13}C MRI was performed with VFA resulting in higher SNR and less imaging blurring.

References [1] Svensson J, et al. MRM 50.2 (2003): 256-262. [2] Reed GD, et al. IEEE Trans Med Imag (2013). [3] Worters PW, et al. MRM 64.5 (2010): 1404-1412. [4] Deppe MH, et al. MRM 67.6 (2012): 1656-1664. [5] Hargreaves BA, et al. MRM 46.1 (2001): 149-158. [6] Scheffler, K, et al, MRM 49.2 (2003): 395-397.